Int. J. Bio-Inorg. Hybr. Nanomater., 5(3): 183-188, Autumn 2016

Quantum mechanical investigation of 4-hydroxy phenyl azobenzene adsorption on the boron nitride nanotubes

F. Azarakhshi, S. Hajibabaie, N. Farhadyar*

Department of Chemistry, Varamin-Pishva Branch, Islamic Azad University, Varamin, Iran

Received: 21 May 2016; Accepted: 24 July 2016

ABSTRACT: In this study, the adsorption of 4-hydroxy phenyl-azobenzene on the surface of (4, 0) zigzag open-end boron nitride nanotube (BNNT) has been investigated by quantum calculations. In order to find the preferred adsorption site, different positions and orientations were considered. The impacts of donor-acceptor electron delocalization on the structural and electronic properties and reactivity of (4, 0) zigzag boron nitride nanotube (BNNT) in interaction with 4-hydroxy phenyl-azobenzene was investigated based on the Density Functional Theory (DFT) calculations. Thermodynamic functional analysis suggesting thermodynamic favourability for adsorption of azo dye on (4, 0) zigzag BNT in both gas and aqueous phases. Delocalization of charge density between the bonding and antibonding orbitals calculated by NBO (natural bond orbital) analysis. In the reaction of BNNT with azo dye, the total electronic energy (E_{el}), azo dye-BNNT dipole moment (5.74 D), resonance energy (E_2), HOMO-LUMO energy bond gaps, density of state (DOS), adsorption energies (ΔE_{Ad}) and structural parameters were calculated.

Keywords: *Adsorption; BNNTs; Density functional theory (DFT); Energy gap; Hydroxy phenyl azobenzene; NBO; Quantum mechanical investigation*

INTRODUCTION

After the discovery of carbon nanotubes, the existence of boron nitride nanotubes (BNNTs) was predicted by Chopra (Chopra, *et al.*, 1995) and Rubio (Rubio, *et al.*, 1994) theoretically based on the structural analogies between the parent materials for CNTs and BNNTs, both being layered materials composed of layers of hexagonal lattices. BNNTs possess excellent mechanical properties, chemical stability and high thermal conductivity (Pouch and Aterovita, 1990, Karnezos, 1990, Blase, *et al.*, 1994 & Wilder, *et al.*, 1998). BNNTs are electrical insulators with a bandgap of 5.5 eV, basically independent of tube chirality and morphology (Blase, *et al.*, 1994). This independence from tube chirality makes boron nitride nanotubes much more tractable. BNNTs are more chemically inert and structurally stable than CNTs. BNNT has semiconductor behaviour that is interesting for applications in nanoscale devices. These kinds of systems are suitable for biological applications (Golberg & Bando, 2001) because they are soluble in water (Huei, *et al.*, 2012) and have prominent anticancer properties provided that they exhibit low toxicity (Raffa, *et al.*, 2012; Ciofani, *et al.*, 2009). Nanotube surface functionalization allows the fabrication of de-

---

(*) Corresponding Author-e-mail: fa_azarakhshi@yahoo.com

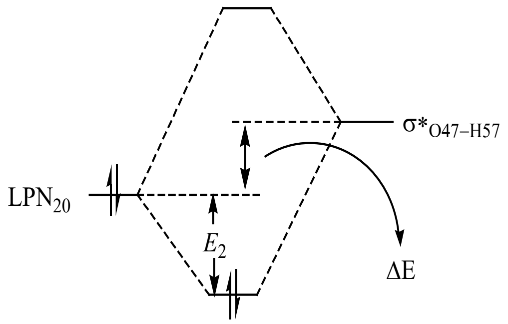

Scheme 1. Schematic representation of the second order perturbation energies (E_2) and the energy gaps between donor and acceptor orbitals in the reaction between BNNT with azo dye

vices such as biosensors (Wu & Yin, 2011) and visible light emitting diodes (Gao, *et al.*, 2011). Taking into account the above mentioned facts it is required to continue exploring the nanotube surface and ends as covalent or non-covalent functionalization with different functional molecules or groups to make electronic properties. Recently adsorption of different molecules toward nanostructures has been studied (Baierle, *et al.*, 2006, Akdim, et al., 2009, Mukhopadhyay, et al., 2010, Krishnakumar & Swaminathan, 2012, Kaur, et al., 2015). There is sufficient published experimental information about the dye removal as environmental pollution from textile wastewater but there is no quantitative theoretical published data about the estereoelectronic effect on the electronic properties and reactivity of boron nitride nanotube (BNNT) in interaction with azo dyes. In this study, (4, 0) zigzag BNNT have been carried out to adsorption of 4-hydroxy phenylazobenzene dye by DFT method. Also, the stereoelectronic orbital interactions and stabilization energies (E_2) associated with electronic delocalization and their influences on the structural properties of azo dye-BNNT were quantitatively.

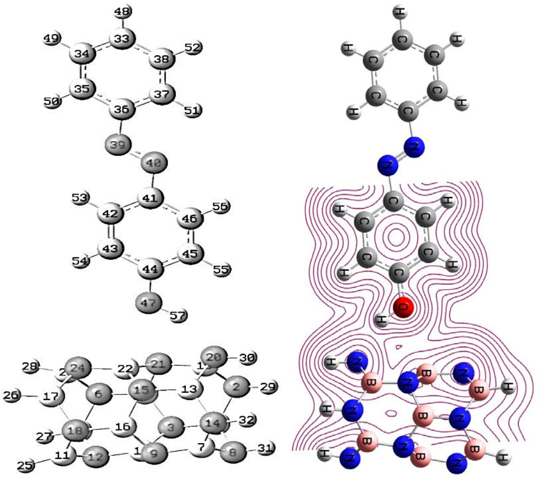

Fig 1. (a) The optimized structure of azo dye-BNNT, (b) The contours shows range of estereoelectronic interactions of azo dye molecule with B12N12H8 nanotube surface

COMPUTATIONAL DETAILS

The structures of B12N12H8 nanotube and azo dye molecules was optimized at the B3LYP/6-31G* level

Table 1. The calculated B3LYP/6-31G* relative energy difference values (ΔE_0), DE$_{Thermal}$ and thermodynamic parameters [ΔH, ΔG (in hartree) and ΔS (in cal mol^{-1} K^{-1})] differences in gas & aqua phases for azo dye-B12N12H8

	ΔG	ΔH	ΔS	ΔE_0	$\Delta E_{Thermal}$
in gas phase	-0.307	-6.972	0.009	-7.643	-6.382
in aqua phase	-0.333	-6.909	0.009	-7.580	-6.317

Table 2. The calculated B3LYP/6-31G* electronic energy values (E_{el}) (in kcal mol^{-1}) for azo Dye, B12N12H8 and azo dye-B12N12H8 and binding energy (BE) (in kcal mol^{-1}) for azo dye-B12N12H8 in gas & aqua phases

Azo dye -B12N12H8	Azo dye	B12N12H8	BE (kcal/mol)
	in gas phase		
-1009620.668	-406613.804	-602998.894	-7.9691
	in aqua phase		
-1009622.237	-406614.118	-603000.149	-7.9692

of theory by using Gaussian quantum chemical package (Frisch, et al., 2004). The B3LYP is commonly used functional in the study of different nanostructures method (Seminario & Politzer, 1995). The vibrational frequencies have been calculated at the same level of theory, which enable us to confirm real minima. NBO analysis was then performed using the B3LYP/6-31G* level for the adsorption interaction of 4-hydroxy phenyl-azobenzene yellow dye on the BNNT by the NBO analysis 5.G program via the PC-GAMESS interface (Glendening, et al., 2004). The stabilization energies associated with electron delocalization are proportional to $S^2/\Delta E$ where S is the orbital overlap and ΔE is the energy differences between the donor and acceptor orbitals. Also, stereoelectronic orbital interactions are anticipated to be more effective for anti rather than the syn or gauche arrangement between the donor and acceptor orbitals, and the stabilization should increase as the acceptor orbital energy decreases and the donor orbital energy increases (Dionne & St-Jacques, 1987, Epiotis, et al., 1977) (Scheme 1):

$$\text{Stabilization or resonance energy } \alpha \ (S^2/\Delta E)$$

RESULTS AND DISCUSSION

Thermodynamic functional analyses on the fully optimized geometries were calculated. The free Gibbs energy (ΔG) and enthalpy (ΔH) values are negative and entropy (ΔS) values are positive, that suggesting thermodynamic favourability for attachment of azo dye on (4, 0) BNNT in both gas and solvent phases (Table 1).

The azo dye molecule has been sat in the different sites to be close to the B12N12H8. The binding energy (BE) of 4-hydroxy phenyl-azobenzene dye on the BNNT is determined through the following equation (1):

$$\Delta E_{adsorption} = \text{Binding Energy}(BE) = E(\text{azo dye} - B12N12H8) - \left[E(\text{azo dye}) + E(B12N12H8)\right] \qquad (1)$$

Where E(azo dye-B12N12H8) is the total energy of the BNNTs interacting with azo dye, E(azo dye) and E(B12N12H8) are total energies of the azo dye and pure BNNT respectively. The binding energy (BE) of 4-hydroxy phenyl-azobenzene dye on the surfaces of BNNT for the optimized structure of azo dye-BNT was calculated -7.969 (kcal/mol) in gas & aqua phases

Table 3. Calculated stabilization (resonance) energies associated with donor-acceptor interactions, off-diagonal elements (a.u.) and orbital energies (a.u.) for azo dye-BNT

azo dye-BNT	E_2	F_{ij}	ΔE
from (BNT) to (azo)			
$\mathbf{LP_1N_{20} \rightarrow \sigma^*_{O47\text{-}H57}}$	16.59	0.102	0.73
$\sigma_{B13\text{-}N20} \rightarrow \sigma^*_{O47\text{-}H57}$	0.43	0.019	1.08
$\sigma_{B19\text{-}N20} \rightarrow \sigma^*_{O47\text{-}H57}$	0.43	0.019	1.08
Σ	**17.45**		
from (azo) to (BNT)			
$\sigma^*_{O47\text{-}H57} \rightarrow LP^*_2B_{22}$	1.15	0.029	0.75
$LP_1O_{47} \rightarrow \sigma^*_{N15\text{-}B22}$	0.94	0.026	0.90
$LP_1O_{47} \rightarrow \sigma^*_{B22\text{-}N24}$	0.43	0.018	0.97
$\mathbf{LP_1O_{47} \rightarrow LP^*_2B_{22}}$	5.60	0.054	0.56
$LP_1O_{47} \rightarrow LP^*_1B_{22}$	0.50	0.019	0.69
$\sigma_{O47\text{-}H57} \rightarrow \sigma^*_{N15\text{-}B22}$	0.36	0.018	1.10
Σ	**8.98**		

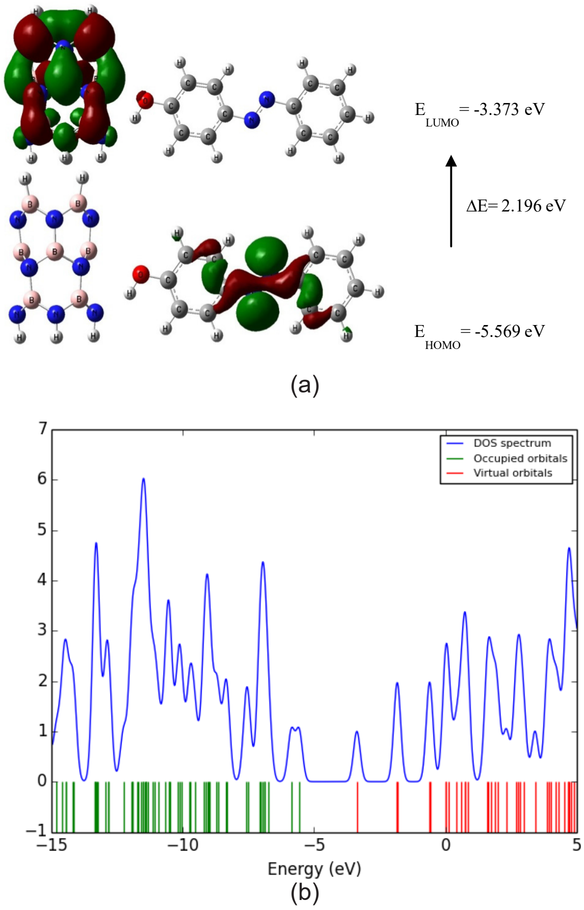

Fig. 2. (a) LUMO and HOMO molecular orbitals of azo dye-B12N12H8, (b) DOS diagram of azo dye-B12N12H8

and results showed that the physical adsorption reaction was occurred (Table 2).

The bonding-antibonding orbital interactions and the stabilization energies (E_2) associated with electron delocalization and their influences on the structural properties of azo dye and BNNT and also, density of state (DOS) were quantitatively investigated by the NBO approach based on B3LYP/6-311+G** level of theory. The NBO analysis showed that the most stabilization energies associated with electron delocalization related to $LP_1N_{20} \rightarrow \sigma^*_{O47-H57}$ and $LP_1O_{47} \rightarrow LP^*_2B_{22}$ for azo dye-boron nitride nanotube compound. Also, there is a direct relationship between the orbital overlap (S) matrix and the off-diagonal elements (F_{ij}). Increase of the off-diagonal elements (F_{ij}) values could increase the $LP_1N_{20} \rightarrow \sigma^*_{O47-H57}$ and $LP_1O_{47} \rightarrow LP^*_2B_{22}$ electron delocalization (Table 3). So the stabilization energies related to electron delocalization are explained the electronic behaviour of azo dye and BNNT during the adsorption reaction.

The stability and reactivity of a molecule relates to energy bond gaps, which means the molecule with least HOMO-LUMO energy gap is more stable because of high electron delocalization between HOMO & LUMO orbitals (Fig. 2). Moreover, the decrease of the bonding orbital occupancies and the increase of

Table 4. B3LYP/6-31G* calculated structural parameters for azo dye, B12N12H8 and azo dye-B12N12H8

Compound	**azo**	Compound	**BNNT**	Compound	**azo-BNNT**
Bond lengths (Å)		Bond lengths (Å)		Bond lengths (Å)	
r_{N7-N8}	1.263	r_{13-15}	1.451	$r_{N39-N40}$	1.263
r_{11-12}	1.405	r_{13-20}	1.474	r_{43-44}	1.407
r_{12-13}	1.399	r_{15-22}	1.477	r_{44-45}	1.402
$r_{C12-O15}$	1.363	r_{22-24}	1.451	$r_{C44-O47}$	1.355
$r_{O15-H25}$	0.970	Bond angles (°)		$r_{O47-H57}$	0.988
Bond angles (°)		$\theta_{15-13-20}$	117.5	r_{13-15}	1.443
θ_{4-7-8}	114.7	$\theta_{13-20-19}$	100.7	r_{13-20}	1.498
θ_{7-8-9}	115.0	$\theta_{19-21-22}$	114.6	r_{15-22}	1.486
$\theta_{11-12-15}$	117.1	$\theta_{21-22-15}$	116.4	r_{22-24}	1.447
$\theta_{13-12-15}$	122.7	$\theta_{21-22-24}$	119.5	Bond angles (°)	
$\theta_{12-15-25}$	109.2	Torsion angles (°)		$\theta_{36-39-40}$	114.7
Torsion angles (°)		$\phi_{13-20-19-21}$	61.1	$\theta_{39-40-41}$	115.1
$\phi_{4-7-8-9}$	180.0	$\phi_{20-19-21-22}$	-21.5	$\theta_{43-44-47}$	117.5
$\phi_{11-12-15-25}$	180.0	$\phi_{21-22-15-13}$	24.3	$\theta_{45-44-47}$	122.6
$\phi_{13-12-15-25}$	0.0	$\phi_{13-15-22-24}$	-179.8	$\theta_{44-47-57}$	112.6
				$\theta_{15-13-20}$	116.6
				$\theta_{13-20-19}$	97.8
				$\theta_{13-15-22}$	114.5
				$\theta_{21-22-15}$	115.1
				$\theta_{21-22-24}$	119.5
				Torsion angles (°)	
				$\phi_{36-39-40-41}$	180.0
				$\phi_{43-44-47-57}$	180.0
				$\phi_{45-44-47-57}$	-0.0
				$\phi_{13-20-19-21}$	64.8
				$\phi_{20-19-21-22}$	-22.7
				$\phi_{21-22-15-13}$	26.5
				$\phi_{13-15-22-24}$	179.5

the anti-bonding orbital occupancies in the BNNTs cause to electron distribution in these compounds.

Representative structural parameters for azo dye, B12N12H8 and azo dye-B12N12H8 are calculated at the B3LYP/6-311+G** level of theory (Table 4). Importantly, the results give evidence that in azo dye-B12N12H8, the $r_{O47-H57}$ bond length is significantly lengthier compared to that in azo dye and the $\theta_{44-47-57}$ and $\theta_{21-22-15}$ bond angles are shorter compared to that in azo dye and B12N12H8 nanotube also, the $\phi_{13-20-19-21}$ and $\phi_{20-19-21-22}$ torsional angles in azo dye-B12N12H8 are lengthier compared to B12N12H8 nanotube. These facts can be explained by the estereoelectronic interactions associated with electron delocalization (see Table 4).

CONCLUSIONS

Bases on the results the BNNTs are effective adsorbents for the dye removal from textile wastewater. Therefore, the investigation of Electronic Behaviour of azo dye- BNNT can provide valuable information about its electronic and structural properties and reactivity of boron nitride nanotubes in interaction with 4-hydroxy phenyl-azobenzene dye. The energy bond gaps show that charge density transfer occurs during the reaction. The binding energy (BE) of 4-hydroxy phenyl-azobenzene dye on the surfaces of BNNT in gas & aqua phases showed that the physical adsorption reaction was occurred.

REFERENCES

Rubio, A., Corkill, J., Cohen, M.L., (1994). Theory of graphitic boron nitride nanotubes. Phys. Rev. B, 49, 5081-5084.

Chopra, N.G., Luyken, R.J., Cherrey, K., Crespi, V.H., Cohen, M.L., Louie, S.G., Zettl, A., (1995). Boron nitride nanotubes. Science, 269, 966-967.

Pouch, J.J., and Aterovita, S.A. eds., (1990). Synthesis and properties of boron nitride. Zurich, Trans Tech. Publications Inc.

Karnezos, M., (1990). Boron-Nitrogen-Hydrogen Thin Films. Mater. Sci. Forum, 54-55, 261-276.

Blase, X., Rubio, A., Louie, S.G., and Cohen, M.L., (1994). Stability and band gap constancy of boron nitride nanotubes. Europhys. Lett., 28, 335-340.

Wilder, J.W.G., Venema, L.C., Rinzler, A.G., Smalley, R.E., and Dekker, C., (1998). Electronic structure of atomically resolved carbon nanotubes. Nature, 391, 59-62.

Golberg, D., Bando, Y., (2001). Unique morphologies of boron nitride nanotubes. Appl. Phys. Lett., 79, 415-417.

Huei Lee, C., Zhang, D., Khin Yap, Y., (2012). Functionalization, dispersion, and cutting of boron nitride nanotubes in water. J. Phys. Chem. C, 116, 1798-1804.

Raffa, V., Riggio, C., Smith, M.W., Jordan, K.C., Cao, W., Cuschieri, A., (2012). BNNT-mediated irreversible electroporation: it's potential on cancer cells. Technol. Cancer Res. Treat, 11, 459-465.

Ciofani, G., Raffa, V., Menciassi, A., Cuschieri, A., (2009). Boron nitride nanotubes: an innovative tool for nanomedicine. Nano Today, 4, 8-10.

Wu, J., Yin, L., (2011). Platinum nanoparticle modified polyaniline functionalized boron nitride nanotubes for amperometric glucose enzyme biosensor. ACS Appl. Mater. Interfaces, 3, 4354-4362.

Gao, Zh., Zhi, Ch., Bando, Y., Golberg, D., Serizawa, T., (2011). Noncovalent functionalization of disentangled boron nitride nanotubes with flavin mononucleotides for strong and stable visible-light emission in aqueous solution. ACS Appl. Mater. Interfaces, 3, 627-632.

Baierle, R.J., Piquini, P., Schmidt, T.M., Fazzio, A., (2006). Hydrogen adsorption on carbon-doped boron nitride nanotubes. J. Phys. Chem. B, 110(42), 21184-21188.

Akdim, B., Kim, S.N., Naik, R.R., Maruyama, B., Pender, M.J., Pachter, R., (2009). Understanding effects of molecular adsorption at a single-wall boron nitride nanotube interface from density functional theory calculations. Nanotechnology, 20, 355705-355712.

Mukhopadhyay, S., Gowtham, S., Scheicher, R.H., Pandey, R., and Karna, Sh.P., (2010). Theoretical Study of Physisorption of Nucleobases on Boron Nitride Nanotubes: A New Class of Hybrid Nano-Bio Materials. Nanotechnology, 21(16), 165703-

165708.

Krishnakumar, B., and Swaminathan, M., (2012). Photodegradation of Acid Violet 7 with AgBr–ZnO under highly alkaline conditions. Spectrochim. Acta Mol. Biomol. Spectrosc., 99, 160-165.

Kaur, J., Singla, P., Goel, N., (2015). Adsorption of oxazole and isoxazole on BNNTs surface: ADFT study. Appl. Surf. Sci., 328, 632-640.

Frisch, M.J., Trucks, G.W., Schlegel, H.B., Scuseria, G.E., Robb, M.A., Cheeseman, J.R., Montgomery, J.A., Vreven, T., Kudin, K.N., Burant, J.C., Millam, J.M., Iyengar, S.S., Tomasi, J., Barone, V., Mennucci, B., Cossi, M., Scalmani, G., Rega, N., Petersson, G.A., Nakatsuji, H., Hada, M., Ehara, M., Toyota, K., Fukuda, R., Hasegawa, J., Ishida, M., Nakajima, T., Honda, Y., Kitao, O., Nakai, H., Klene, M., Li, X., Knox, J.E., Hratchian, H.P., Cross, J.B., Bakken, V., Adamo, C., Jaramillo, J., Gomperts, R., Stratmann, R.E., Yazyev, O., Austin, A.J., Cammi, R., Pomelli, C., Ochterski, J.W., Ayala, P.Y., Morokuma, K., Voth, G.A., Salvador, P., Dannenberg, J.J., Zakrzewski, V.G., Dapprich, S., Daniels, A.D., Strain, M.C., Farkas, O., Malick, D.K., Rabuck, A.D., Raghavachari, K., Foresman, J.B., Ortiz, J.V., Cui, Q., Baboul, A.G., Clifford, S., Cioslowski, J., Stefanov, B.B., Liu, G., Liashenko, A., Piskorz, P., Komaromi, I., Martin, R.L., Fox, D.J., Keith, T., Al-Laham, M.A., Peng, C.Y., Nanayakkara, A., Challacombe, M., Gill, P.M.W., Johnson, B., Chen, W., Wong, M.W., Gonzalez, C., Pople, J.A., (2004). Gaussian 03, Revision B.03, Gaussian, Inc., Wallingford CT.

Seminario, J.M., and Politzer, P. (Eds(., (1995). Modern Density Function Theory, a Tool for Chemistry. Elsevier, Amsterdam.

Glendening, E.D., Badenhoop, J.K., Reed, A.E., Carpenter, J.E., Bohmann, J.A., Morales, C.M., Weinhold, F., (2004). Theoretical Chemistry Institute, University of Wisconsin, Madison , WI, NBO Version 5.G.

Dionne, P., and St-Jacques, M., (1987). Mechanism of the gauche conformational effect in 3-halogenated 1,5-benzodioxepins. J. Am. Chem. Soc., 109, 2616-2623.

Epiotis, N.D., Yates, R.L., Larson, R.J., Kirmayer, C.R., Bernardi, F., (1977). Directional effects of sigma. Conjugation on geometrical isomerism. J. Am. Chem. Soc., 99, 8379-8388.

AUTHOR (S) BIOSKETCHES

Fatemeh Azarakhshi, Assistant Professor, Department of Chemistry, Varamin-Pishva Branch, Islamic Azad University, Varamin, Iran, *E-mail: fa_azarakhshi@yahoo.com*

Samaneh Hajibabaie, M.Sc., Department of Chemistry, Varamin-Pishva Branch, Islamic Azad University, Varamin, Iran

Nazanin Farhadyar, Associate Professor, Department of Chemistry, Varamin-Pishva Branch, Islamic Azad University, Varamin, Iran